JOURNAL OF VIROLOGY, Sept. 1996, p. 6278–6287 Vol. 70, No. 9
0022-538X/96/$04.00+0

Cell Proteins Bind Specifically to West Nile Virus Minus-Strand 3′ Stem-Loop RNA

PEI-YONG SHI,† WEI LI, AND MARGO A. BRINTON*
Department of Biology, Georgia State University, Atlanta, Georgia 30303

Received 18 January 1996/Accepted 30 May 1996

The first 96 nucleotides of the 5′ noncoding region (NCR) of West Nile virus (WNV) genomic RNA were previously reported to form thermodynamically predicted stem-loop (SL) structures that are conserved among flaviviruses. The complementary minus-strand 3′ NCR RNA, which is thought to function as a promoter for the synthesis of plus-strand RNA, forms a corresponding predicted SL structure. RNase probing of the WNV 3′ minus-strand stem-loop RNA [WNV (−)3′SL RNA] confirmed the existence of a terminal secondary structure. RNA-protein binding studies were performed with BHK S100 cytoplasmic extracts and in vitro-synthesized WNV (−)3′SL RNA as the probe. Three RNA-protein complexes (complexes 1, 2, and 3) were detected by a gel mobility shift assay, and the specificity of the RNA-protein interactions was confirmed by gel mobility shift and UV-induced cross-linking competition assays. Four BHK cell proteins with molecular masses of 108, 60, 50, and 42 kDa were detected by UV-induced cross-linking to the WNV (−)3′SL RNA. A preliminary mapping study indicated that all four proteins bound to the first 75 nucleotides of the WNV 3′ minus-strand RNA, the region that contains the terminal SL. A flavivirus resistance phenotype was previously shown to be inherited in mice as a single, autosomal dominant allele. The efficiencies of infection of resistant cells and susceptible cells are similar, but resistant cells (C3H/RV) produce less genomic RNA than congenic, susceptible cells (C3H/He). Three RNA-protein complexes and four UV-induced cross-linked cell proteins with mobilities identical to those detected in BHK cell extracts with the WNV (−)3′SL RNA were found in both C3H/RV and C3H/He cell extracts. However, the half-life of the C3H/RV complex 1 was three times longer than that of the C3H/He complex 1. It is possible that the increased binding activity of one of the resistant cell proteins for the flavivirus minus-strand RNA could result in a reduced synthesis of plus-strand RNA as observed with the flavivirus resistance phenotype.

Flaviviruses are single-stranded RNA viruses with positive-polarity RNA genomes of approximately 11 kb (44). The genome contains a single, long open reading frame. The encoded polyprotein is translated and co- and posttranslationally processed by viral and cellular proteases into three structural (capsid, membrane, and envelope) proteins and seven nonstructural (NS1, NS2a, NS2b, NS3, NS4a, NS4b, and NS5) proteins (13). The functions of the seven nonstructural proteins are not well understood. Upon infection, the plus-strand genomic RNA is transcribed into a complementary minus-strand RNA, which in turn serves as the template for the transcription of plus-strand genomic RNA. During the flavivirus replication cycle, the synthesis of plus- and minus-strand RNAs is disproportionate; about 10 to 100 times more plus-strand RNA than minus-strand RNA is produced (52).

The terminal 5′ and 3′ noncoding regions (NCRs) of the West Nile virus (WNV) genome RNA are 96 and 580 nucleotides (nt) long, respectively (13). Previous studies have indicated that the 3′ and 5′-terminal nucleotides of the flavivirus genome can form conserved stem-loop (SL) structures (10, 11, 13). The SL structure formed by the 3′-terminal nucleotides is more stable than the structure formed by the 5′-terminal nucleotides. The conservation of terminal structures and short sequence elements within these structures among divergent flaviviruses suggests that they may function as *cis*-acting signals for the initiation of viral RNA replication or translation. Partial or complete deletion of the sequences forming the terminal structures has been shown to be lethal for infectious flavivirus clones (12, 32).

The results of an analysis of the components of purified viral replication complexes of several RNA viruses have suggested that host factors are functional components of their replicase complexes. In studies with Qβ phage, three host proteins and one viral protein were found in the viral replication complex (33), while one host protein and two viral proteins were found in purified cucumber mosaic virus replication complexes (22). A host protein was also detected in purified Sindbis virus replication complexes (3). It was recently reported that poliovirus preinitiation RNA replication complexes formed in an in vitro replication system require soluble cellular factors for the synthesis of VPg-linked viral RNA (2).

Specific binding of host cell proteins to regions within the 3′ and 5′ NCRs of a number of animal RNA virus genomes has been reported. Three cytoplasmic proteins have been shown to bind to the 3′ SL structures of the rubella virus genome RNA (37, 38). Only one of these proteins and two additional proteins bind specifically to the 3′ end of the rubella virus minus-strand RNA (37). Cell proteins have also been shown to bind specifically to the 3′ ends of mouse hepatitis virus minus-strand RNA (16), Sindbis virus minus-strand RNA (39, 40), measles virus plus-strand RNA (34), and poliovirus and rhinovirus genomic RNAs (26, 54). For both rubella virus and mouse hepatitis virus, it has been reported that different cellular proteins bind to the 3′ end of the minus-strand RNA and to the complementary 5′ end of the plus-strand RNA (16, 43). We have recently reported that three BHK cell proteins (105, 84,

* Corresponding author. Mailing address: Department of Biology, Georgia State University, University Plaza, Atlanta, GA 30303. Phone: (404) 651-3113. Fax: (404) 651-2509. Electronic mail address: biomab@panther.gsu.edu.
† Present address: Department of Biophysics and Biochemistry, Yale University School of Medicine, New Haven, CT 06520.

and 56 kDa) bind specifically to the 3′ SL structures of WNV and dengue type 3 virus genomic RNAs (5, 5a).

Flavivirus-resistant mice were first reported in the early 1920s, when Webster (57) demonstrated that individuals within a stock of randomly bred mice varied greatly in their susceptibility to louping ill virus. Resistance to flavivirus-induced morbidity and mortality was subsequently shown to be inherited as a single dominant allele (36, 58). This gene, now designated *Flv*, has been mapped to murine chromosome 5 (47). The flavivirus resistance gene has been identified not only in laboratory mice but also in populations of wild mice in both the United States (15a) and Australia (46). Resistant mice are susceptible to flavivirus infection, but the yield of virus from resistant animals, as well as from cultured cells obtained from them, is significantly lower than that from susceptible animals or cells (17). The spread of infection in resistant mice is slower, which allows the host immune response to efficiently clear the infection (15a, 17). Although factors such as the age of the host, the degree of virulence of the infecting flavivirus, the route of infection, and immunosuppression can result in a lethal infection in resistant mice (8, 45), the minimal lethal dose of virus required for resistant mice is always 10 to 100 times higher than that for susceptible mice, the day of death for resistant mice is delayed by 3 or more days, and the brain virus titers for resistant mice are always 1,000 to 10,000-fold lower than those for susceptible mice (15a, 17, 21, 56a). Virus yields from cell cultures of the resistant and susceptible cells differ by 100- to 1,000-fold (7, 15). The tissue from which cell cultures are prepared does not appear to be important, since brain, kidney, macrophage, and embryo fibroblast cultures from resistant animals all produced reduced flavivirus yields (56). Congenic strains of homozygous resistant (C3H/RV) and susceptible (C3H/He) mice have been developed (19), and transformed lines of embryo fibroblasts have been established (15). Comparison of the various stages of the flavivirus replication cycle in resistant C3H/RV and susceptible C3H/He cells showed that the synthesis of progeny genome RNA (plus strand), but not replicative-form/replicative-intermediate RNA, was specifically limited in resistant cells (6, 7). In addition, deleted viral RNAs with homologous interfering activity are preferentially amplified by resistant cells (7, 48). These data suggest that the flavivirus resistance gene product acts intracellularly at the level of viral RNA synthesis.

In this study, we confirm the existence of an SL structure at the 3′ end of the WNV minus-strand RNA and identify four proteins that interact specifically with this RNA in BHK, C3H/He, and C3H/RV cell extracts. Comparison of RNA-protein complexes from flavivirus-resistant and -susceptible cells showed that the half-life of complex 1 from resistant cells is three times longer than the half-life of the complex 1 from susceptible cells.

MATERIALS AND METHODS

Cells and virus. BHK-21/WI2 cells (referred to hereafter as BHK cells) (55), C3H/He and C3H/RV cell lines (15) were used to prepare infected and uninfected cytoplasmic extracts. The C3H/He and C3H/RV cell lines were derived from congenic flavivirus-susceptible and -resistant mouse strains, respectively, as described previously (15). To prepare infected extracts, confluent BHK monolayers were infected with WNV strain E101 at a multiplicity of infection of 1 as described previously (11). Infected-cell extracts were harvested 24 h after infection as described below.

Preparation of cell extracts. Cell extracts were prepared as described previously (5) with some modifications. Briefly, cells were grown to confluency in T-150 tissue culture flasks. The monolayers were washed three times with cold phosphate-buffered saline (PBS), scraped from the flask with a rubber policeman, and pelleted by centrifugation at 160 × *g* for 4 min at 4°C. The cell pellets were washed twice with cold PBS and repelleted. The cell pellets were resuspended in cytolysis buffer (10 mM *N*-2-hydroxyethylpiperazine-*N*′-2-ethanesulfonic acid [HEPES] [pH 7.9], 5 mM dithiothreitol, 10 mM NaCl, 0.1 mM phenylmethylsulfonyl fluoride, 10 μg of leupeptin [Boehringer Mannheim Biochemicals] per ml, 1% Triton X-100, 20% glycerol) at 5.0×10^7 cells per ml, vortexed for 15 s, and allowed to sit on ice for 15 min. The cell lysates were centrifuged at 2,000 × *g* for 4 min at 4°C to remove the nuclei, and the supernatant was then centrifuged at 100,000 × *g* for 45 min at 4°C. The resulting supernatant (S100) was concentrated, and the buffer was exchanged with storage buffer (20 mM HEPES [pH 7.5], 100 mM NaCl, 2 mM $MgCl_2$, 5 mM dithiothreitol, 50% glycerol) in a Centricon-30 microconcentrator as described by the manufacturer (Amicon). The total protein concentration of each extract was determined with the bicinchoninic acid assay (Pierce). Protein concentrations ranged from 1 to 3 μg/μl. Cell extracts were stable for 2 weeks at −20°C.

Construction of plasmids. Virion RNA was isolated and gradient purified as described previously (6). The complete 96-nt 5′ NCR and the first 261 nt of the adjacent capsid gene were amplified from purified WNV genome RNA via reverse transcription-PCR using the anti-genomic-sense primer 1 (5′-CTAGTT CTTTCTTGAAACTC-3′), located between genome nt 367 to 348, and the genomic-sense primer 2 (5′-GAGTAGTTCGCCTGTTGAG-3′), located from nt 1 to 18 at the 5′ end of the WNV genomic RNA. The PCR product was directly cloned into the pCR1000 plasmid (Invitrogen) via the TA cloning method to generate plasmid p5′NCR-C. From the p5′NCR-C clone, two subclones, p75nt(−)3′ and p96nt(−)3′, were constructed via PCR amplification using a genomic-sense primer identical to primer 2, except that it contained a 5′ tail with a *Hin*dIII site, and one of two forward primers (negative-sense primers, from nt 54 to 75 or from nt 96 to 75), each with a tail containing an *Apa*I restriction site. The PCR products were digested with *Apa*I and *Hin*dIII and cloned into a similarly digested pCR1000 vector. pCR1000 was chosen as the vector because the *Apa*I site in this vector is positioned adjacent to the T7 promoter, thus minimizing the number of additional nonviral nucleotides on the 5′ end of the minus-strand RNA transcribed from this template. The subclone, p320nt(−)3′, was generated by a similar PCR protocol using a primer identical to primer 2, except that it contains an *Eco*RI site on the 5′ end and primer 3 (negative-sense primer, from nt 207 to 320) with a *Hin*dIII site on the 5′ end. pGEM3 (Promega) was used as the vector for this construct because an *Apa*I cutting site was present within the p320nt(−)3′ sequence. The constructs were transfected into strain DH5α of *Escherichia coli*, and colonies were selected and sequenced to ensure that no mutation had occurred during the subcloning procedures. Plasmid DNA was purified from *E. coli* DH5α with a plasmid purification kit (Qiagen) and analyzed on agarose gels prior to use as templates for RNA transcription.

In vitro transcription of ^{32}P-labeled RNA probes. Purified p75nt(−)3′, p96nt(−)3′, and p350nt(−)3′ DNAs were linearized with *Hin*dIII and then transcribed with T7 RNA polymerase to yield WNV 75nt(−)3′SL, WNV 96nt(−)3′SL, and WNV 350nt(−)3′SL RNA, respectively. The in vitro transcription reaction mixture (20 μl) was incubated at 37°C for 1 h and contained 40 mM Tris-HCl (pH 7.9), 6 mM $MgCl_2$, 10 mM NaCl, 2 mM spermidine, 10 mM dithiothreitol, 0.5 μM ribonucleotides (ATP, CTP, and GTP; Boehringer Mannheim Biochemicals), 12 μM UTP, 50 μCi of [α-^{32}P]UTP (3,000 Ci/mmol; Amersham), 80 U of T7 RNA polymerase (Ambion), 1 μg of DNA template, and 20 U of RNasin (Boehringer Mannheim Biochemicals). After ethanol precipitation, the ^{32}P-labeled RNAs were resuspended in 10 μl of loading buffer (7 M urea and 0.025% bromophenol blue) and electrophoresed on an 8% polyacrylamide gel containing 7 M urea. The gel was autoradiographed, and the RNA was eluted from excised gel slices overnight at room temperature in a solution containing 0.5 M ammonium acetate, 0.5% sodium dodecyl sulfate (SDS), and 1 mM EDTA. The eluted RNA was filtered through a 0.45-μm-pore-size cellulose acetate filter unit (Costar Co.) to remove gel pieces, extracted with phenol-chloroform, aliquoted, precipitated with ethanol, and stored at −70°C.

In vitro synthesis of unlabeled RNA competitors. Two of the unlabeled competitor RNAs were transcribed in vitro in a 100-μl reaction mixture containing 80 mM HEPES (pH 7.5), 14 mM $MgCl_2$, 2 mM spermidine, 10 mM dithiothreitol, 750 μmol of ribonucleotides (ATP, GTP, CTP, and UTP), 100 U of RNasin, 5 μg of DNA template, and 100 U of T7 RNA polymerase at 37°C for 2.5 h. The RNA transcripts were electrophoresed on denaturing 8% polyacrylamide gels. The unlabeled RNA bands were located following autoradiography by comparison to a few lanes containing the same RNA labeled with [^{32}P]UTP. The unlabeled RNAs were eluted from the gel slices as described above.

Four different nonspecific RNAs were used. Plasmid pCR1000 was linearized with *Eco*RI and transcribed to yield a 92-nt RNA which contains the cloning cassette of this vector. D10 RNA was synthesized in vitro from a 90-bp PCR product that contains the T7 promoter sequence followed by the 67-bp template for the U1 stem II and D10 epitope as described elsewhere (4). The plasmid used for D10 RNA synthesis was a kind gift from J. Keene (Duke University, Durham, N.C.). D10 RNA, yeast tRNA (Gibco BRL Life Technologies), and pCR1000 RNA were chosen because they contain an SL structure and are similar in length to or shorter than the WNV 96nt(−)3′SL RNA. Poly(I)-poly(C) was obtained from Boehringer Mannheim Biochemicals.

RNase structure probing. Purified WNV 75nt(−)3′SL RNA was treated with calf intestinal alkaline phosphatase (Boehringer Mannheim Biochemicals) to remove the 5′ phosphate and ethanol precipitated. The dephosphorylated RNA was 5′ end labeled by incubation with [γ-^{32}P]ATP (3,000 Ci/mmol; Amersham) and T4 polynucleotide kinase (Promega) at 37°C for 10 min as described by the

manufacturer and then repurified on an 8% denaturing gel and eluted as described above. The labeled RNA was precipitated with ethanol using tRNA (10 μg) as a coprecipitate and stored at −80°C. RNase probing was performed by the method of Knapp (29) with modifications. Briefly, the 5′-end ^{32}P-labeled RNA was pelleted, washed with 70% ethanol, dried in a Speed-vac, and dissolved in RNA renaturing buffer (20 mM HEPES [pH 7.6], 200 mM NaCl, 1 mM dithiothreitol, 10 mM $MgCl_2$). The RNA was quantitated by measuring radioactivity with a scintillation counter (model LS6500; Beckman) in Ready Solv HP fluid (Beckman). For each experiment, RNA concentrations were adjusted to 5×10^4 cpm of RNA per 20 μl of renaturing buffer. The RNA was renatured by incubation at 85°C for 2 min, slowly cooled to room temperature, and placed in an ice bath. Prior to RNase digestion, 0.15 mg of tRNA per ml was added and the RNA sample was aliquoted at 2 μl per tube. The double-strand-specific RNase cobra venom nuclease V1 (RNase V1) (8.75×10^{-3}, 1.75×10^{-2}, or 3.5×10^{-2} U/ml; Pharmacia) or one of three single-strand-specific RNases, RNase A (1.25×10^{-3}, 2.5×10^{-2}, or 5×10^{-1} μg/ml; Boehringer Mannheim Biochemicals), RNase T_1 (2.5×10^{-2}, 5×10^{-2}, or 10^{-1} μg/ml; Boehringer Mannheim Biochemicals), or RNase PhyM (0.25, 0.5, or 1 U/ml; Pharmacia), was added to the RNA at the concentrations indicated. The reaction mixtures were incubated in an ice bath for 20 min or at room temperature for 16 min, and then 2 μl of sample buffer (10 M urea, 10% glycerol, 0.05% xylene cyanol, 0.05% bromophenol blue) was added. All digested RNA samples were analyzed on 10% polyacrylamide sequencing gels.

An alkaline hydrolysis ladder was generated as previously described (29). Briefly, WNV 75nt(−)3′SL RNA (10^4 cpm) was dissolved in 4 μl of hydrolysis buffer (50 mM $NaHCO_3$-Na_2CO_3 [pH 9.2]), 1 μg of tRNA per μl was added, and the RNA was incubated at 90°C for 6 min and immediately placed in an ice-slurry bath. RNA sequencing reactions were performed by incubating 7×10^3 cpm of RNA in 4 μl of sequencing buffer (20 mM sodium citrate [pH 5.0], 1 mM EDTA, 7 M urea, 0.025% xylene cyanol, 0.025% bromophenol blue, and 1 μg of tRNA per μl) with 0.01 U of RNase T_1 per μl, 0.1 U of RNase U2 per μl, or 2.5×10^{-4} U of RNase A per μl. The reactions were terminated by placing them in an ice bath and were immediately loaded onto a sequencing gel.

CD spectroscopy. The circular dichroism (CD) spectrum of the WNV 75nt(−)3′SL RNA was measured with a Jasco-J710 spectropolarimeter, equipped with a programmable Neslab temperature controller as previously described (61). Cylindrical cuvettes with a path length of 1 cm were used. Spectra were recorded from 350 to 200 nm and averaged over five scans. RNA samples were prepared in a buffer consisting of 5 mM Na_2HPO_4 (pH 7.0), 0.1 mM EDTA, and 100 mM NaCl.

Thermal melting curves. Absorbance-versus-temperature melting curves of the WNV 75nt(−)3′SL RNA were measured at 260 nm with a heating rate of 0.5°C min^{-1} on a Cary 4 spectrometer as described previously (28). RNA samples were prepared in the same buffer as described for CD spectroscopy. The derivatives of the melting curves were taken with a five-point parabolic fit with binomial weighing at each temperature.

Gel mobility shift assay of RNA-protein interactions. Uniformly labeled RNA probe (5,000 cpm, approximately 0.3 ng), 1 μg of S100 cytoplasmic extract, and 7 μg of poly(I)-poly(C) in a final volume of 10 μl of binding buffer (5 mM HEPES [pH 7.5], 25 mM KCl, 2 mM $MgCl_2$, 0.1 mM EDTA, 2 mM dithiothreitol, 3.8% glycerol) were incubated at 30°C for 10 min. The RNA probes were renatured in binding buffer as described above prior to use in these assays. For gel shift competition experiments, various amounts of unlabeled RNA were added to the binding reaction mixture either simultaneously with or at various times after the ^{32}P-labeled probe. The reaction mixture was then electrophoresed on a 6.5% nondenaturing polyacrylamide gel made in 0.5× Tris-borate-EDTA containing 2.5% glycerol. The polyacrylamide gel was prerun at 120 V for 15 min, and electrophoresis was performed at 120 V at room temperature. The gel was dried and autoradiographed. The densities of the RNA-protein complex bands were quantitated with a densitometer (Molecular Dynamics) in some experiments.

UV-induced cross-linking of RNA-protein complexes. A ^{32}P-labeled RNA (10,000 cpm) probe was incubated with 2 μg of S100 cell extract and 12 μg of poly(I)-poly(C) in a final volume of 20 μl of binding buffer at 30°C for 10 min and then irradiated with a 254-nm-wavelength UV lamp (Ultra-violet Products, Inc.) held 3 cm from the light source on ice for 30 min (38). After irradiation, the samples were incubated with RNase T_1 (20 U) and RNase A (20 μg) for 12 min at room temperature, boiled for 3 min in Laemmli sample buffer (28), and electrophoresed on an SDS–10% polyacrylamide gel.

Preparation of figures. All figures containing data obtained by autoradiography were generated by computer imaging, using Adobe Photoshop, version 2.5, after the X-ray films were scanned with an Agfa Arcus 2 flatbed scanner.

RESULTS

RNase structure probing of the WNV (−)3′SL RNA. It was previously reported on the basis of thermodynamic folding predictions that a conserved terminal SL structure could be formed by the WNV 5′ NCR. This structure was conserved among flavivirus genomic RNAs, even though their sequences diverged significantly (10). A corresponding SL structure can be formed by the minus-strand 3′ RNA, which is complementary to the plus-strand 5′ NCR sequence. The predicted terminal SL structure is formed by nt 4 to 74 of the WNV 3′ minus-strand RNA. To test whether the predicted secondary structure exists, the WNV 75nt(−)3′SL RNA was subjected to RNase structure probing analysis. In vitro-transcribed, 5′-end-labeled WNV 75nt(−)3′SL RNA was subjected to limited digestion under native conditions with either a double-strand-specific RNase (V1) or one of three single-strand-specific RNases (A, T_1, or PhyM) as described in Materials and Methods, and the digestion products were analyzed on a 10% polyacrylamide sequencing gel. An autoradiograph of a representative experiment is shown in Fig. 1A, and a summary of the RNase cleavage data obtained from the experiments performed is presented in Fig. 1B. Both weak and strong RNase cleavages are indicated on the thermodynamically predicted SL structure. RNases A and PhyM strongly digested nt 30 to 35. Nucleotides 24 to 27 and 38 to 42 were strongly cleaved by RNase V1, while RNase V1 weakly cleaved nt 23 and 37. These results support the existence of the predicted SL at the top of the structure (Fig. 1B). The observed RNase A cleavage at nt 13 to 19 and nt 21 and 22 and the RNase A, PhyM, or T_1 cleavages at nt 43 to 44 and 47 to 62 suggest that the predicted base pairing in the middle of the structure does not exist. Instead, the regions consisting of nt 13 to 22 and 43 to 62 form a large internal loop. The region consisting of nt 65 to 67 and nt 11 and 12 was sensitive to digestion by RNase V1. G-A base pairs have been reported in both RNA and DNA structures (18, 23, 53, 60). Potential G-A base pairs could be formed between the A's at positions 12 and 67 and the G's at positions 65 and 11, respectively. Also, purine stacking is possible between the G's at positions 64 and 65 and at positions 10 and 11. RNase V1 cleavage of nt 5 to 10 and 68 to 74 indicates the existence of the predicted bottom stem region (Fig. 1B).

CD and thermal melting spectroscopic analysis of WNV (−)3′SL RNA. The conformation and thermostability of the WNV 75nt(−)3′SL RNA were further analyzed by CD and thermal melting spectroscopy. The CD spectra indicated the presence of a highly structured RNA conformation with a significant amount of A-form helix. At temperatures above 90°C, the CD spectra were typical of an unstructured single-stranded RNA (data not shown).

To obtain thermal transitions of the WNV 75nt(−)3′SL RNA, we carried out a series of thermal melting studies and a reversible, complex UV-visible melting curve with significant hyperchromicity was obtained. As illustrated in Fig. 2A, broad low-temperature transitions were followed by a sharper high-temperature transition. The derivative curve (Fig. 2B) of the same experiment as shown in Fig. 2A indicated that there were two partially resolved overlapping transitions with peaks at around 36 and 47°C and a high-temperature transition at 83°C. Both the CD and thermal melting data indicate that the WNV 75nt(−)3′SL RNA contains a highly ordered structure with a significant level of A-form helix.

BHK cell proteins that bind to the WNV (−)3′SL RNA. Gel mobility shift assays were performed to detect proteins that can interact specifically with the 3′ NCR of WNV genomic RNA. ^{32}P-labeled WNV 96nt(−)3′SL RNA was incubated with either a WNV-infected or uninfected BHK S100 cytoplasmic extract, and the resulting RNA-protein complexes were electrophoresed on a native polyacrylamide gel. Poly(I)-poly(C) (7 μg) was added to the binding reaction mixture to reduce nonspecific RNA-protein interactions. An extra band was often observed in the free probe lane on nondenaturing mobility shift gels. Only a single species of the RNA was detected on a

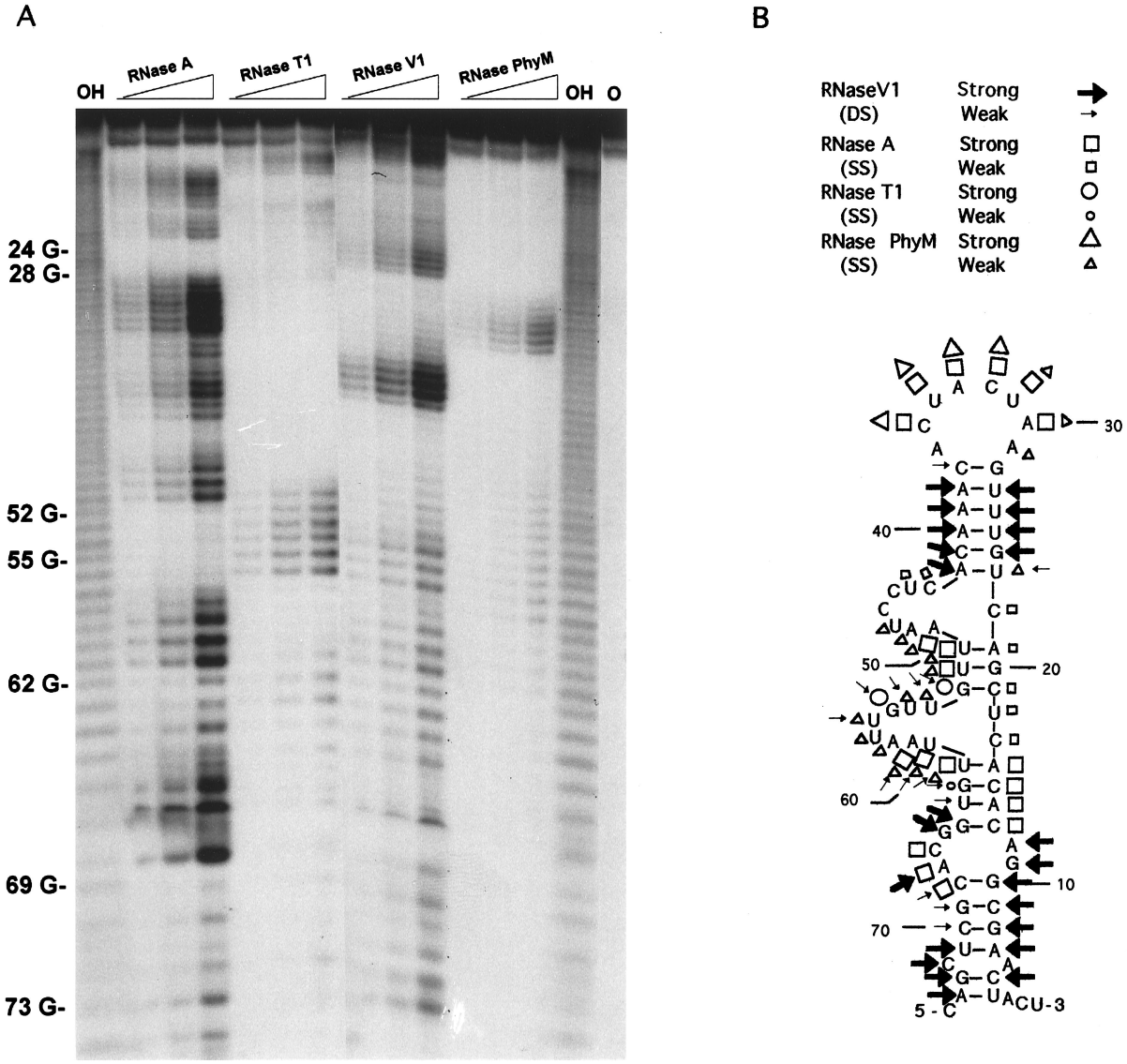

FIG. 1. RNase probing of the first 75 3′-terminal nucleotides of the WNV minus-strand RNA. (A) 5′ ^{32}P-labeled WNV 75nt(−)3′SL RNA was digested under native conditions with increasing amounts of one of three single-strand-specific RNases, RNase A, T_1, or PhyM, or with the double-strand-specific RNase V1. The cleavage products were separated on a 10% polyacrylamide sequencing gel. RNA sequencing reaction mixtures (data not shown) and alkaline hydrolysis ladders were used as markers. Lanes OH, alkaline hydrolysis ladder; lane O, no nuclease treatment. The numbers to the left of the gel are the nucleotide positions. (B) Summary of RNase cleavage data. Both strong and weak RNase cleavages are indicated on the computer-predicted secondary structure. The nucleotides are numbered from the 3′ end of the minus-strand RNA. DS, double strand; SS, single strand.

polyacrylamide gel containing 7 M urea and on a nondenaturing gel after heating and cooling the RNA under dilute conditions (data not shown). These data suggest that the RNA in this band is most likely a multimer or a different conformer of the probe (Fig. 3). The RNA in the multimer band does not participate in the formation of RNA-protein complexes, since the density of this band did not decrease upon the addition of cell extract. With uninfected BHK cell extracts, three RNA-protein complexes (complexes 1, 2, and 3) were detected (Fig. 3, lane U). Three complexes with electrophoretic mobilities identical to those detected in uninfected extracts were observed when WNV-infected BHK cell extracts were incubated with the WNV 96nt(−)3′SL RNA (Fig. 3, lane I). Preliminary results from both probe titration and complex dissociation rate experiments also indicated that there were no differences between the proteins obtained from infected and uninfected cells (data not shown). These results suggest that only cellular proteins are involved in the formation of the three complexes that were detected by this assay. Thus, uninfected-cell extracts were used in the majority of the subsequent experiments.

Specificity of the RNA-protein interactions. Gel mobility shift competition assays were performed with unlabeled specific competitor or with one of four nonspecific competitors. When increasing amounts of the unlabeled specific competitor (25, 50, 75, 100, 150, 200, 250, or 300 ng) were added to the binding reaction mixtures, decreasing amounts of each of the RNA-protein complexes were observed (Fig. 4A, lanes 3 to 10). When either 300 or 600 ng of one of the nonspecific competitors, plasmid RNA, D10 RNA, tRNA, or poly(I)-poly(C), was added to the binding reaction mixture, essentially no competition with complex formation was detected with any of the nonspecific competitors (Fig. 4B), indicating that the

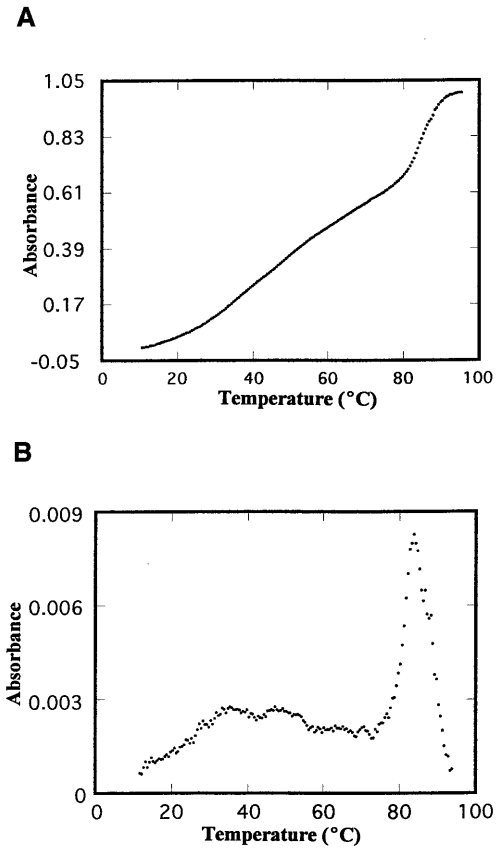

FIG. 2. Thermal melting spectra of the WNV 75nt(−)3′SL RNA. (A) Thermal melting curve of the WNV 75nt(−)3′SL RNA. (B) Derivative curve of the thermal melting curve of the WNV 75nt(−)3′SL RNA. Three transitions are easily visible in the derivative plot.

binding of the cellular proteins to the WNV 96nt(−)3′SL RNA was specific. Also, no competition in gel mobility shift assays was observed when the terminal 96 nt of the WNV (+)3′SL RNA was used as a competitor (data not shown). Because of the complementarity of the WNV (+)5′SL RNA to the WNV (−)3′SL RNA, this RNA was not used as a competitor.

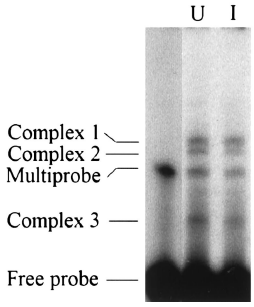

FIG. 3. Comparison of RNA-protein complexes formed between the 3′-terminal region of the WNV minus-strand RNA and proteins in S100 extracts from WNV-infected or uninfected BHK cells. Infected BHK cell extracts were harvested 20 h after infection with WNV at a multiplicity of infection of 1. ^{32}P-labeled WNV 96nt(−)3′SL RNA was incubated with cell extract for 10 min at 30°C. The binding reaction mixtures were then analyzed on a 6.5% nondenaturing polyacrylamide gel. Lane U, uninfected BHK cells; lane I, infected BHK cells; unlabeled lane, free probe.

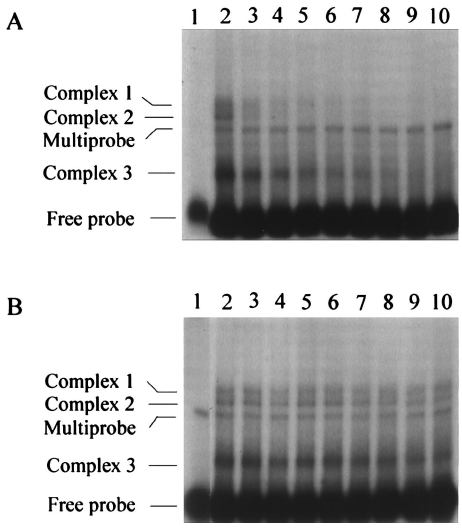

FIG. 4. Gel mobility shift competition assay of the RNA-protein complexes formed with the 3′-terminal region of the WNV minus-strand RNA. ^{32}P-labeled WNV 96nt(−)3′SL RNA was incubated with an uninfected BHK cell extract for 10 min at 30°C in the presence or absence of various amounts of unlabeled competitor RNAs. (A) Competition with unlabeled specific RNA competitor. Lane 1, free probe; lane 2, no competitor; lanes 3 to 10, increasing amounts of unlabeled specific RNA (25, 50, 75, 100, 150, 200, 250, and 300 ng, respectively) were added to the binding reaction mixtures. (B) Competition with unlabeled nonspecific RNA competitors. Lane 1, free probe; lane 2, no competitor; lanes 3 to 10, various unlabeled nonspecific RNAs [tRNA (lanes 3 and 4), D10 RNA (lanes 5 and 6), poly(I)-poly(C) (lanes 7 and 8), and plasmid RNA (lanes 9 and 10)] at 300 or 600 ng, respectively, were added to the binding reaction mixture as indicated.

Determination of the molecular masses of the WNV (−)3′SL RNA-binding proteins in BHK cytoplasmic extracts. UV-induced cross-linking was performed with the labeled WNV 96nt(−)3′SL RNA as the probe. The RNA-protein complexes were irradiated with UV light to covalently cross-link the RNA to the proteins. Unbound regions of the probe RNA were digested with RNases A and T_1. The UV-induced cross-linked proteins were electrophoresed on an SDS-polyacrylamide gel and were detected by autoradiography. Four proteins of approximately 108, 60, 50, and 42 kDa were observed (Fig. 5A, lane U). No ^{32}P-labeled protein bands were detected if the cell extract was excluded (Fig. 5A, lane C1) or if a complete reaction mixture was not exposed to UV irradiation (Fig. 5A, lane C2).

Although three RNA-protein complexes with identical mobilities were detected with both uninfected- and infected-cell extracts, it is possible that different protein components involved in the complexes from infected and uninfected cells. To rule out this possibility, UV-induced cross-linking assays were carried out with WNV-infected cell extracts. Four cellular proteins with identical molecular masses were detected with either uninfected- or infected-cell extracts (Fig. 5B, lanes U and I). This result further supports the hypothesis that the proteins involved in the formation of the three detected RNA-protein complexes are cellular and not viral proteins.

To further demonstrate the specificity of these RNA-protein interactions, competition UV-induced cross-linking experiments were performed. Complex formation with the 60-, 50-, and 42-kDa proteins was inhibited by small amounts of specific competitor but not by substantially larger amounts of two nonspecific competitors (Fig. 5C). A larger amount of specific competitor (1.2 μg) was required to observe competition with the 108-kDa protein. At the same concentration, the plasmid

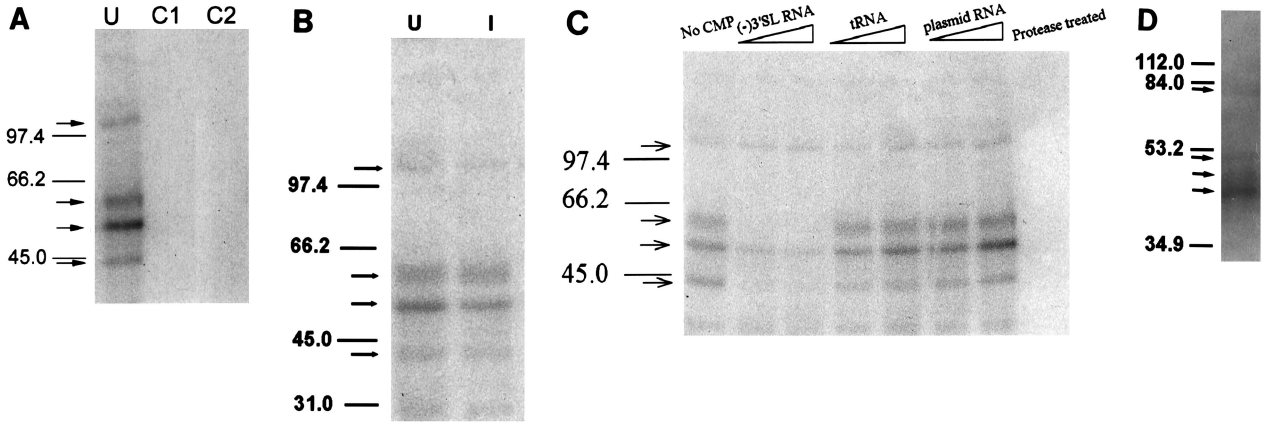

FIG. 5. Detection of proteins in S100 BHK cell extracts that bind to the WNV (−)3′SL RNA or to the WNV (+)5′SL RNA. ^{32}P-labeled WNV 96nt(−)3′SL RNA or 96nt(+)5′SL RNA was incubated with BHK cell extracts and then subjected to UV-induced cross-linking. The samples were then digested with an RNase cocktail (RNases A and T_1) and analyzed by SDS-polyacrylamide gel electrophoresis. (A) UV cross-linking of WNV 96nt(−)3′SL RNA with uninfected BHK cell extracts. Four cellular proteins (42, 50, 60, and 108 kDa) were covalently cross-linked to the WNV 96nt(−)3′SL RNA (lane 1). No ^{32}P-labeled bands were detected in a reaction mixture without cell extract (lane C1) or in a reaction mixture containing cell extract but with no UV irradiation (lane C2). (B) Comparison of UV-induced cross-linking of WNV 96nt(−)3′SL RNA with either uninfected (lane U) or WNV-infected (lane I) BHK cell extracts. Four cellular proteins with similar mobilities were covalently cross-linked to the WNV 96nt(−)3′SL RNA. (C) Analysis of the specificity of proteins detected by UV-induced cross-linking. UV-induced cross-linking competition assays were performed in the presence of increasing amounts of the competitor RNAs (from left to right as indicated by the triangles above the lanes): WNV(−)3′SL RNA, 25 and 75 ng; tRNA or plasmid RNA, 100 and 600 ng. Lane No CMP, no competitor RNA added; lane protease treated, protease treated-cytoplasmic extracts were pretreated with proteinase K (2 μg/ml, 37°C for 15 min) prior to use in the cross-linking assay. (D) UV-induced cross-linking of WNV 96nt(+)5′SL RNA with uninfected BHK cell extracts. Four proteins (69, 38, 40, and 45 kDa) with mobilities different from those observed with WNV 96nt(−)3′SL RNA were detected. The positions of molecular mass markers (in kilodaltons) are shown to the left of the gels. Cross-linked proteins are indicated by arrows.

RNA gave no competition, but some competition was observed with the tRNA. We reported previously that unlabeled WNV (−)3′SL RNA inhibited the formation of complexes between the 105-kDa protein and the WNV (+)3′SL RNA probe approximately 4.5 times more efficiently than did unlabeled WNV (+)3′SL RNA (5). Both the previous and the present results appear to indicate that the p105/108 protein binds to the WNV (−)3′SL RNA with a high affinity. However, further data are required to confirm this hypothesis. Unfortunately, the UV-induced cross-linking assay is not sensitive enough for use in measuring protein binding affinities, especially when the protein is present in a crude cytoplasmic extract. Therefore, further analysis of the binding characteristics of this protein will have to be postponed until the protein has been purified.

Detection of cellular proteins that bind to the WNV (+)5′SL RNA. The sequence of the 5′ NCR of the genomic RNA is complementary to that of the minus-strand 3′ NCR RNA, and both sequences can form similar SL structures. To determine whether cell proteins also bind to the WNV (+)5′SL RNA, UV-induced cross-linking was carried out using the WNV 96nt(+)5′SL RNA as the probe. Four cellular proteins (69, 45, 40, and 38 kDa) were detected (Fig. 5D). The molecular masses of these four proteins were different from those of the four proteins detected with the complementary WNV (−)3′SL RNA. As a control, ^{32}P-labeled plasmid RNA was used as the probe in a UV-induced cross-linking experiment performed under the same conditions, and no cross-linked proteins were detected with this RNA (data not shown).

Preliminary mapping of the protein binding sites on the WNV (−)3′SL RNA. The RNA probe used in the previous UV-induced cross-linking experiments contained the entire 3′ NCR (96 nt) of the minus-strand 3′ RNA. Since the terminal SL structure is formed by the first 75 nt of the 3′ minus strand, it is possible that this region of the RNA contains all the sequence and/or structural elements necessary to bind the four cellular proteins detected with the WNV 96nt(−)3′SL RNA. To test this possibility, UV-induced cross-linking was performed with the WNV 75nt(−)3′SL RNA as the probe (Fig. 6, lane 3). The same four cellular proteins were detected with the WNV 96nt(−)3′SL and the 75nt(−)3′SL RNAs (Fig. 6, lanes 2 and 3, respectively), indicating that the binding sites for the four proteins are located within the 3′-terminal 75 nt of the minus-strand RNA.

To determine whether additional 5′ sequence would affect the binding of the four proteins to the terminal SL, a WNV 320nt(−)3′SL RNA, which contains the complete 3′ NCR and the adjacent 5′ portion of the capsid gene, was used as the probe in a UV-induced cross-linking assay. The same four cellular proteins were cross-linked to the WNV 320nt(−)3′SL RNA (Fig. 6, lane 1) as to the two shorter probes. In order to obtain sharp bands after UV-induced cross-linking, 3.5 times more RNase was required for the WNV 320nt(−)3′SL RNA than for the 96nt(−)3′SL RNA probe. Even so, RNase-resistant RNA fragments were still present at the bottom of the gel.

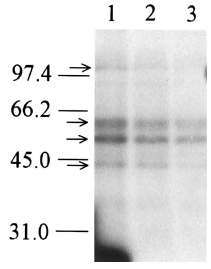

FIG. 6. Comparison of proteins in S100 BHK cell extracts that bind to WNV (−)3′SL RNAs of different lengths. One of three ^{32}P-labeled probes [WNV 320nt(−)3′SL RNA (lane 1), WNV 96nt(−)3′SL RNA (lane 2), and WNV 75nt(−)3′SL RNA (lane 3)] was incubated with a BHK cell extract and then subjected to UV-induced cross-linking. Four cellular proteins (arrows) migrating in an identical pattern were covalently cross-linked to each of the minus-strand 3′-terminal RNAs. The positions of molecular mass markers (in kilodaltons) are shown to the left of the gel.

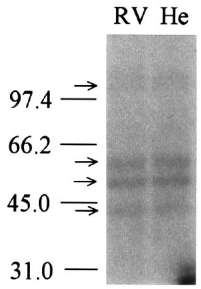

FIG. 7. Comparison of proteins binding to the WNV (−)3′SL RNA in flavivirus-resistant (C3H/RV) and susceptible (C3H/He) cell extracts. ^{32}P-labeled WNV 96nt(−)3′SL RNA was cross-linked to proteins in C3H/RV and C3H/He cell extracts. Four cellular proteins (arrows) with the same mobility patterns were cross-linked with either resistant (lane RV) or susceptible (lane He) cell extracts. The pattern of cellular proteins detected was the same as that observed with BHK cell extracts. The positions of molecular mass markers (in kilodaltons) are shown to the left of the gel.

The relative intensities of the protein bands decreased as the length of the probe decreased, even though the amounts of RNase (RNase T_1 and A) used in the cross-linking experiments were proportional to the lengths of the probes [three-fourths of the amount of RNase was used for the digestion of the UV-cross-linked WNV 75nt(−)3′SL RNA compared with the amount used for the UV-cross-linked WNV 96nt(−)3′SL RNA]. It is possible that cross-linked WNV 75nt(−)3′SL RNA is more accessible to RNase digestion than cross-linked WNV 96nt(−)3′SL or 320nt(−)3′SL RNA, resulting in shorter ribonucleotide fragments with fewer labeled nucleotides remaining attached to the cross-linked proteins. The additional 5′ sequence could increase the stability of the 3′SL by providing tertiary interactions. A similar observation was recently reported for the 3′ plus-strand RNA of rhinovirus 14 (54).

Comparison of RNA-protein complex formation by C3H/RV and C3H/He cell extracts. A single, dominant gene, designated *Flv*, confers resistance to flavivirus-induced disease in mice (7, 15a, 45, 58). Resistance is specific to flaviviruses and occurs at the level of genome RNA replication. We hypothesize that the less efficient genome RNA replication observed in resistant cells could be the result of a mutation in one of the host proteins that binds to the (−)3′SL RNA template during the initiation of plus-strand RNA viral transcription. UV-induced cross-linking was used to compare the cell proteins that bound to the WNV 96nt(−)3′SL RNA probe in flavivirus-resistant (C3H/RV) and flavivirus-susceptible (C3H/He) murine cell extracts. Four cellular proteins with identical electrophoretic mobilities were detected in both C3H/He and C3H/RV cell extracts (Fig. 7). The calculated molecular masses of the four cross-linked proteins in both types of murine cells were also the same as those detected by the WNV 96nt(−)3′SL RNA in BHK cell extracts (Fig. 5A). No significant differences in the densities of any of the cross-linked cellular protein bands were detected between the C3H/He and C3H/RV cell extracts (Fig. 7), indicating that the same relative amounts of the proteins were present. However, the densities of all four protein bands detected in both types of murine cells were consistently lower than those of the bands detected in the BHK cells when the same amount of total protein was utilized from each species in UV-induced cross-linking experiments. This may be due to lower levels of these proteins in the murine extracts, to differences in their binding activity resulting from sequence variation, or to differences in the levels or the binding activities of competing cell factors. Interestingly, WNV has previously been reported to replicate less efficiently in mouse cells than in hamster cells (6).

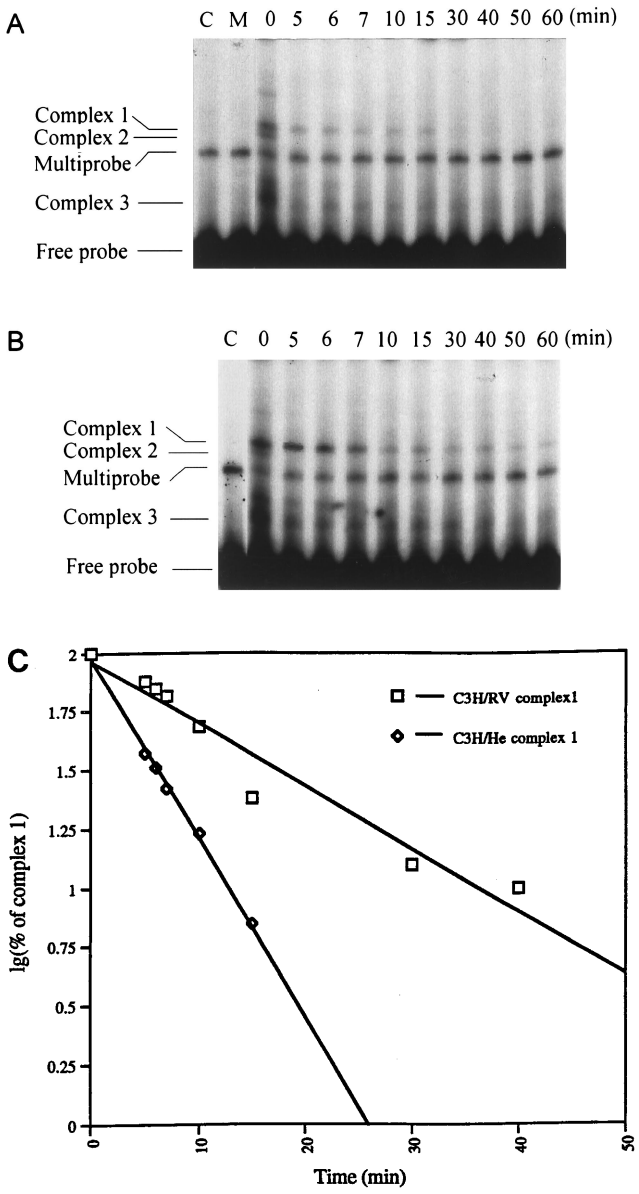

FIG. 8. Comparison of the half-life of RNA-protein complexes formed with resistant (C3H/RV) and susceptible (C3H/He) cell proteins. RNA-protein complexes were formed by incubating the ^{32}P-labeled WNV (−)3′SL RNA with an S100 extract from either C3H/RV or C3H/He cells. An excess of unlabeled WNV (−)3′SL RNA was then added. After the indicated periods of incubation, the reaction mixtures were electrophoresed on 6.5% nondenaturing polyacrylamide gels, and the RNA-protein complexes were quantitated with a PhosphorImager. (A) Time course of C3H/He RNA-protein complex dissociation. (B) Time course of C3H/RV RNA-protein complex dissociation. Lane M, free probe; lane C, reaction mixture in which competitor and probe were added simultaneously. (C) Dissociation kinetics of C3H/He and C3H/RV RNA-protein complexes. lg, logarithm.

The RNA-protein complexes formed by the C3H/He and C3H/RV cell extracts were also compared. Three RNA-protein complexes with electrophoretic mobilities identical to those detected with BHK cell extracts were observed with both C3H/He and C3H/RV extracts. However, more of the complex 1 band was formed with C3H/RV extracts than with C3H/He extracts (compare lane 0 in Fig. 8A with lane 0 in Fig. 8B). To

further characterize differences in RNA-protein complex formation between the C3H/He and C3H/RV extracts, the half-life of each of the RNA-protein complexes was determined as described by Pardigon and Strauss (39). RNA-protein complexes were formed by incubating ^{32}P-labeled 96nt(−)3′SL RNA with a cell extract for 10 min, and then an excess amount of unlabeled specific competitor was added. After various periods of further incubation time (as indicated in Fig. 8) in the presence of the unlabeled specific competitor (150 ng), the RNA-protein complexes remaining were electrophoresed on a native polyacrylamide gel and detected by autoradiography (Fig. 8). When the same amount of unlabeled specific competitor RNA (150 ng) was added to the cell extracts at the same time as the ^{32}P-labeled WNV 96nt(−)3′SL probe, all of the labeled complexes were eliminated (Fig. 8A, lane C, and Fig. 8B, lane C). The densities of the ^{32}P-labeled complexes were quantitated with a PhosphorImager and plotted against the time that the preformed complexes were incubated with the specific competitor (Fig. 8C). The half-life ($t_{1/2}$) of a complex is equal to the time required for the unlabeled specific competitor to eliminate 50% of the ^{32}P-labeled RNA-protein complex. A dramatic difference in the $t_{1/2}$ values of complex 1 from the C3H/He and C3H/RV extracts was observed; the $t_{1/2}$ values for complex 1 were approximately 3.5 min when formed with C3H/He extracts and 12 min when formed with C3H/RV extracts. The $t_{1/2}$ of complex 3 formed with C3H/RV extracts is 1.5 times longer than the $t_{1/2}$ of complex 3 formed with C3H/He extracts. In contrast, similar $t_{1/2}$ values were obtained with both types of cell extracts for complex 2. These results demonstrate that complex 1 and to a lesser degree complex 3 formed by C3H/He cell extracts dissociate faster than the complexes 1 and 3 formed by C3H/RV cell extracts.

DISCUSSION

CD and thermal melting analyses indicated that the WNV 75nt(−)3′SL RNA is highly structured with a significant amount of A-form helix. The existence of a 3′-terminal SL structure in the WNV minus-strand RNA was further supported by the data obtained by RNase probing (Fig. 1). The WNV (−)3′SL RNA structure appears to contain a large internal loop. Data obtained with longer segments of the WNV (−)3′ RNA suggest that the terminal 3′ structure may be stabilized by tertiary interactions with downstream sequences. Further studies are required before an accurate model for this RNA structure can be drawn.

Cytoplasmic proteins from both hamster and mouse cells were shown to bind specifically to the 3′-terminal 75 nt of the WNV minus-strand RNA. UV-induced cross-linking studies showed that the molecular masses of the proteins detected in all three cell extracts were 42, 50, 60, and 108 kDa. We have previously demonstrated that three BHK cytoplasmic proteins (56, 84, and 105 kDa) bind specifically to the 3′-terminal SL structures of the genomic RNAs of WNV, dengue type 3 virus, yellow fever virus, and tick-borne encephalitis virus (5, 5a). In addition, it was shown that the 105-kDa protein binds to both the WNV (+)3′SL RNA and the WNV (−)3′SL RNA. In competition assays, the WNV (−)3′SL RNA inhibited the formation of complexes between the 105-kDa protein and a WNV (+)3′SL RNA probe approximately 4.5 times more efficiently than did the WNV (+)3′SL RNA (5). The 108-kDa protein detected by UV-induced cross-linking with the WNV (−)3′SL RNA is likely to be the 105-kDa protein detected with the WNV (+)3′SL RNA. Similarly, in the rubella virus system, one of the cell proteins binds to both the rubella plus- and minus-strand 3′SL RNAs (38). In flavivirus-infected cells, the level of plus-strand RNA synthesis is 10 to 100 times greater than that of minus-strand synthesis (14, 52). The different efficiencies of RNA transcription from the flavivirus plus- and minus-strand templates may in part be regulated through the utilization of different sets of cell proteins for the initiation of transcription from the two viral template RNAs. The 105-kDa protein could provide a function that is required to initiate both 3′ ends, possibly a protein-protein interaction with the viral polymerase or helicase. However, the precise functional contributions of individual cell proteins to flavivirus RNA replication remain to be elucidated. The different RNA structures present at the 3′ ends of the flavivirus plus- and minus-strand RNAs may also be involved in regulating the efficiency of RNA synthesis.

None of the proteins which bind to the WNV (−)3′SL RNA were found to bind to the complementary WNV (+)5′SL RNA. Similarly, different sets of proteins were found to bind to the 5′ end of the plus-strand RNA and the 3′ end of the minus-strand RNA of both rubella virus and mouse hepatitis virus (16, 38). This finding is not surprising, since the 5′ end of the genome is involved in translation initiation and possibly also interactions with the capsid protein, while the 3′ end of the minus strand is involved in the initiation of plus-strand synthesis. The localization of the binding regions for the four proteins to the 3′-terminal SL of the WNV minus strand suggests that they may play a role in the initiation of plus-strand RNA transcription. The gel shift and UV-induced cross-linking patterns obtained with uninfected and WNV-infected cell extracts were identical, suggesting that the initial interaction of the viral template RNA may be with cellular proteins rather than viral proteins. Interactions between cell proteins and the viral 3′ SL RNA may result in conformational changes in both the viral RNA and the bound cell proteins. Such conformational changes could be a prerequisite for recognition of the complex by the viral polymerase.

Since flaviviruses can replicate efficiently in mammalian, avian, insect, reptile, and amphibian hosts as well as in cell cultures from these various hosts (8), it would be expected that the domains in the cell proteins that bind to the 3′-terminal regions of the flavivirus RNAs would be highly conserved and present in the cells of all species that are susceptible to flavivirus replication. To date, we have found that the four proteins that bind to the WNV (−)3′SL RNA are identical in size in cells from two rodent species, the hamster and the mouse. Studies are currently under way to determine whether cell proteins that can bind to flavivirus 3′ RNAs are also present in other host species that are susceptible to flavivirus infection.

Analysis of the dissociation rates of the RNA-protein complexes formed between cell proteins and the WNV minus-strand 3′ RNA indicated that complex 1 from the C3H/RV cells had a $t_{1/2}$ that was three times longer than that of the complex 1 from C3H/He cells. No differences in $t_{1/2}$s were observed between any of the complexes formed by the WNV plus-strand 3′ RNA with extracts from resistant and susceptible cells (5a). The flavivirus genetic resistance phenotype has been mapped to a single locus and has been shown to preferentially decrease the synthesis of new plus-strand viral RNA in the infected resistant cells. If one of the proteins that binds to the flavivirus (−)3′SL RNA is the product of the resistance gene, then sequence differences between the resistant and susceptible allele products could result in the observed difference in their binding affinities for the flavivirus (−)3′SL RNA. Since no differences were observed in the sizes of the four proteins detected by the WNV (−)3′SL RNA in C3H/RV and C3H/He extracts (Fig. 7), sequence differences between the products of the two alleles would likely be base substitutions or small

deletions, insertions, or rearrangements. It would be expected that proteins that are involved in the formation of a viral RNA transcription initiation complex would bind to the 3′ end of a viral template RNA in a reversible manner. Therefore, the effect of a mutation that increases the affinity of binding would likely be to reduce the efficiency of progeny RNA transcription initiation and possibly also to lower the rate of progression of the polymerase complex. Pardigon and Strauss (40) previously reported that a single-nucleotide deletion located near the 3′ end of the Sindbis virus minus-strand RNA was lethal for the virus. An RNA probe containing this deletion bound to the same cell proteins as the wild-type probe. However, the $t_{1/2}$ of the RNA-protein complex formed with the mutant probe was three times longer than that of the complex formed with the wild-type probe. Thus, mutations in either the viral RNA or one of the cell proteins that binds to the viral RNA may have a significantly adverse effect on viral RNA synthesis. A study has been initiated to further characterize the cell proteins that bind to the WNV (−)3′SL RNA as a means of testing the hypothesis that one of these proteins is the product of the flavivirus resistance gene.

Resistance at the intracellular level has also been demonstrated for influenza virus (20, 25), mouse hepatitis virus (1, 59), and retroviruses (27). Both the mouse hepatitis virus resistance gene and the influenza virus resistance gene, *Mx*, have been shown to segregate independently of the flavivirus resistance gene in C3H mice. The *Mx* gene, which confers resistance to influenza A virus infection in both mice and cell culture, is inherited as a single dominant gene (35), as is the flavivirus resistance gene. However, expression of the influenza A virus resistance gene product is induced by alpha interferon, while expression of the flavivirus resistance gene product is not (9, 24). The inducibility of the Mx protein by interferon facilitated the rapid cloning and sequencing of this gene (25, 49, 50). Although the product of the murine *Mx* gene has been characterized for some time (50), the mechanism by which the Mx protein specifically interferes with influenza virus replication is not yet understood. Initial experiments suggested that the murine Mx1 protein acted to inhibit influenza virus at the level of viral mRNA synthesis (30, 41, 42). One study showed that the inhibitory effect of the Mx1 protein on influenza virus replication could be overcome by overexpression of the three influenza virus polymerase proteins, PB1, PB2, and PA, and to a lesser extent by expression of the PB2 protein alone, suggesting that the Mx1 protein interacts with a component of the influenza virus polymerase complex (25a). It has been hypothesized that the Mx1 protein may form a complex with PB2, thus preventing PB2 from binding to the other polymerase components or the template RNA. Alternatively, Mx1 may compete with the PB2 protein for its normal site on the viral polymerase complex (51). Intracellular resistance to influenza virus appears to be dependent on host factor interactions with viral proteins, while the flavivirus resistance mechanism appears to depend on host factor interactions with viral RNA.

ACKNOWLEDGMENTS

We thank W. David Wilson and Jerry Blackwell for their many contributions to this work.

This work was supported by Public Health Service research grant AI 18382 from the National Institute of Allergy and Infectious Diseases. Purchase of the DNA synthesizer, model 381 (Applied Biosynthesis, Foster City, Calif.), was funded by the Georgia Research Alliance.

REFERENCES

1. **Bang, F., and A. Warwick.** 1960. Mouse macrophages as host cells for the mouse hepatitis virus and the genetic basis of their susceptibility. Proc. Natl. Acad. Sci. USA **46:**1065–1075.
2. **Barton, D. J., E. P. Black, and J. B. Flanegan.** 1995. Complete replication of poliovirus in vitro: preinitiation RNA replication complexes require soluble cellular factors for the synthesis of VPg-linked RNA. J. Virol. **69:**5516–5527.
3. **Barton, D. J., S. G. Sawicki, and D. L. Sawicki.** 1991. Solubilization and immunoprecipitation of alphavirus replication complexes. J. Virol. **65:**1496–1506.
4. **Bentley, R. C., and J. D. Keene.** 1991. Recognition of U2 small nuclear RNAs can be altered by a 5-amino-acid segment in the U2 small nuclear ribonucleoprotein particle (snRNP) B″ and through interactions with U2 snRNP-A′ protein. Mol. Cell. Biol. **11:**1829–1839.
5. **Blackwell, J. L., and M. A. Brinton.** 1995. BHK cell proteins that bind to the 3′ stem-loop structure of the West Nile virus genome RNA. J. Virol. **69:**5650–5658.

5a. **Blackwell, J. L., and M. A. Brinton.** Unpublished data.

6. **Brinton, M. A.** 1981. Isolation of a replication-efficient mutant of West Nile virus from a persistently infected genetically resistant mouse cell culture. J. Virol. **39:**413–421.
7. **Brinton, M. A.** 1983. Analysis of extracellular West Nile virus particles produced by cell cultures from genetically resistant and susceptible mice indicates enhanced amplification of defective interfering particles by resistant cultures. J. Virol. **46:**860–870.
8. **Brinton, M. A.** 1986. Replication of flaviviruses, p. 329–376. *In* S. Schlesinger and M. Schlesinger (ed.), The viruses. The Togaviridae and Flaviviridae. Plenum Publishing Corp., New York.
9. **Brinton, M. A., H. Arnheiter, and O. Haller.** 1982. Interferon independence of genetically controlled resistance to flaviviruses. Infect. Immun. **36:**284–288.
10. **Brinton, M. A., and J. H. Dispoto.** 1988. Sequence and secondary structure analysis of the 5′-terminal region of flavivirus genome RNA. Virology **162:**290–299.
11. **Brinton, M. A., A. V. Fernandez, and J. H. Dispoto.** 1986. The 3′-nucleotides of flavivirus genomic RNA form a conserved secondary structure. Virology **153:**113–121.
12. **Cahour, A., A. Pletnev, M. Vazeille-Falcoz, L. Rosen, and C.-J. Lai.** 1995. Growth-restricted dengue virus mutants containing deletions in the 5′ noncoding region of the RNA genome. Virology **207:**68–76.
13. **Chambers, T. J., C. S. Hahn, R. Galler, and C. M. Rice.** 1990. Flavivirus genome organization, expression, and replication. Annu. Rev. Microbiol. **44:**649–688.
14. **Cleaves, G. R., T. E. Ryan, and R. W. Schlesinger.** 1981. Identification and characterization of type 2 dengue virus replicative intermediate and replicative form RNAs. Virology **111:**73–83.
15. **Darnell, M. B., and H. Kaprowski.** 1974. Genetically determined resistance to infection with group B arboviruses. II. Increased production of interfering particles in cell cultures from resistant mice. J. Infect. Dis. **129:**248–256.

15a. **Darnell, M. B., H. Koprowski, and K. Lagerspetz.** 1974. Genetically determined resistance to infection with group B arboviruses. I. Distribution of the resistance gene among various mouse populations and characteristics of gene expression *in vivo*. J. Infect. Dis. **129:**240–247.

16. **Furuya, T., and M. M. C. Lai.** 1993. Three different cellular proteins bind to complementary sites on the 5′-end-positive and 3′-end-negative strands of mouse hepatitis virus RNA. J. Virol. **67:**7215–7222.
17. **Goodman, G. T., and H. Koprowski.** 1962. Study of the mechanism of innate resistance to virus infection. J. Cell. Comp. Physiol. **59:**333–342.
18. **Green, K. L., R. L. Jones, Y. Li, H. Robinson, A. H. Wang, G. Zon, and W. D. Wilson.** 1994. Solution structure of a GA mismatch DNA sequence, d(CC ATGAATGG)2, determined by 2D NMR and structural refinement methods. Biochemistry **33:**1053–1062.
19. **Groshel, D., and H. Koprowski.** 1965. Development of a virus-resistant inbred mouse strain for the study of innate resistance to arbo B viruses. Arch. Gesamte Virusforsch. **18:**379–391.
20. **Haller, O.** 1981. Inborn resistance of mice to orthomyxoviruses. Curr. Top. Microbiol. Immunol. **92:**25–52.
21. **Hanson, B., and H. Koprowski.** 1969. Interferon-mediated natural resistance of mice to arbo B virus infection. Microbios **1B:**51–68.
22. **Hayes, R. J., and K. W. Buck.** 1990. Complete replication of a eukaryotic virus RNA *in vitro* by a purified RNA-dependent RNA polymerase. Cell **63:**363–368.
23. **Heus, H. A., and A. Pardi.** 1991. Structural features that give rise to the unusual stability of RNA hairpins containing GNRA loops. Science **253:**191–194.
24. **Horisberger, M. A., O. Haller, and H. Arnheiter.** 1980. Interferon-dependent genetic resistance to influenza virus in mice: virus replication in macrophages is inhibited at an early step. J. Gen. Virol. **50:**205–210.
25. **Horisberger, M. A., P. Staeheli, and O. Haller.** 1983. Interferon induces a unique protein in mouse cells bearing a gene for resistance to influenza virus. Proc. Natl. Acad. Sci. USA **80:**1910–1914.

25a. **Huang, T., J. Pavlovic, P. Staeheli, and M. Krystal.** 1992. Overexpression of the influenza virus polymerase can titrate out inhibition by the murine Mx1 protein. J. Virol. **66:**4154–4160.

26. **Jacobson, S. J., D. A. M. Konings, and P. Sarnow.** 1993. Biochemical and genetic evidence for a pseudoknot structure at the 3′ terminus of the polio-

virus RNA genome and its role in viral RNA amplification. J. Virol. **67:** 2961–2971.
27. **Jolicoeur, P.** 1979. The *Fv-1* gene of the mouse and its control of murine leukemia virus replication. Curr. Top. Microbiol. Immunol. **86:**67–122.
28. **Kibler-Herzog, L., B. Kell, G. Zon, K. Shinozuka, S. Mizan, and W. D. Wilson.** 1990. Sequence dependent effects in methylphosphonate deoxyribonucleotide double and triple helical complexes. Nucleic Acids Res. **18:**3545–3555.
29. **Knapp, G.** 1989. Enzymatic approaches to probing of RNA secondary and tertiary structure. Methods Enzymol. **180:**192–212.
30. **Krug, R. M., M. Shaw, B. Broni, G. Shapiro, and O. Haller.** 1985. Inhibition of influenza viral mRNA synthesis in cells expressing the interferon-induced *Mx* gene product. J. Virol. **56:**201–206.
31. **Laemmli, U. K.** 1970. Cleavage of structural proteins during the assembly of the head of bacteriophage T4. Nature (London) **227:**680–685.
32. **Lai, C.-J., R. Men, M. Pethel, and M. Bray.** 1992. Infectious RNA transcribed from stably cloned full-length cDNA: construction of growth-restricted dengue virus mutants, p. 265–270. *In* F. Brown, R. M. Chanock, H. S. Ginsberg, and R. A. Lerner (ed.), Vaccine 92. Cold Spring Harbor Laboratory Press, Cold Spring Harbor, N.Y.
33. **Landers, T. A., T. Blumenthal, and K. Weber.** 1974. Function and structure in ribonucleic acid phage Qβ ribonucleic acid replicase. J. Biol. Chem. **249:**5801–5808.
34. **Leopardi, R., V. Hukkanen, R. Vainionpää, and A. A. Salmi.** 1993. Cell proteins bind to sites within the 3′ noncoding region of the positive-strand leader sequence of measles virus RNA. J. Virol. **67:**785–790.
35. **Lindenmann, J.** 1964. Inheritance of resistance to influenza virus in mice. Proc. Soc. Exp. Biol. **116:**506–509.
36. **Lynch, C. J., and T. P. Hughes.** 1936. The inheritance of susceptibility to yellow fever encephalitis in mice. Genetics **21:**104–112.
37. **Nakhasi, H. L., X. Q. Cao, T. A. Rouault, and T. Y. Lui.** 1991. Specific binding of host cell proteins to the 3′-terminal stem-loop structure of rubella virus negative-strand RNA. J. Virol. **65:**5961–5967.
38. **Nakhasi, H. L., T. A. Rouault, D. J. Haile, T. Y. Lui, and R. D. Klausner.** 1990. Specific high-affinity binding of host cell proteins to the 3′ region of rubella virus RNA. New Biol. **2:**255–264.
39. **Pardigon, N., E. Lenches, and J. H. Strauss.** 1993. Multiple binding sites for cellular proteins in the 3′ end of Sindbis alphavirus minus-sense RNA. J. Virol. **67:**5003–5011.
40. **Pardigon, N., and J. H. Strauss.** 1992. Cellular proteins bind to the 3′ end of Sindbis virus minus-strand RNA. J. Virol. **66:**1007–1015.
41. **Pavlovic, J., O. Haller, and P. Staeheli.** 1992. Human and mouse Mx proteins inhibit different steps of the influenza virus multiplication cycle. J. Virol. **66:**2564–2569.
42. **Pavlovic, J., T. Zürcher, O. Haller, and P. Staeheli.** 1990. Resistance to influenza virus and vesicular stomatitis virus conferred by expression of human MxA protein. J. Virol. **64:**3370–3375.
43. **Pogue, G. P., X. Q. Cao, N. K. Singh, and H. L. Nakhasi.** 1993. 5′ sequences of rubella virus RNA stimulate translation of chimeric RNAs and specifically interact with two host-encoded proteins. J. Virol. **67:**7106–7117.
44. **Rice, C. M., E. M. Lenches, S. R. Eddy, S. J. Shin, R. L. Sheets, and J. H. Strauss.** 1985. Nucleotide sequence of yellow fever virus: implications for flavivirus gene expression and evolution. Science **229:**726–735.
45. **Sabin, A. B.** 1952. Genetic, hormonal, and age factors in natural resistance to certain viruses. Ann. N. Y. Acad. Sci. **54:**936–944.
46. **Sangster, M. Y., and G. R. Shellam.** 1986. Genetically controlled resistance to flaviviruses within the house mouse complex of species. Curr. Top. Microbiol. Immunol. **127:**313–318.
47. **Sangster, M. Y., N. Urosevic, J. P. Mansfield, J. S. Mackenzie, and G. R. Shellam.** 1994. Mapping the *Flv* locus controlling resistance to flaviviruses on mouse chromosome 5. J. Virol. **68:**448–452.
48. **Smith, A. L.** 1981. Genetic resistance to lethal flavivirus encephalitis: effect of host age and immune status and route of inoculation on production of interfering Banzi virus in vitro. Am. J. Trop. Med. Hyg. **30:**1319–1323.
49. **Staeheli, P., R. J. Colonno, and Y.-S. E. Cheng.** 1983. Different mRNAs induced by interferon in cells from inbred mouse strains A/J and A2G. J. Virol. **47:**563–567.
50. **Staeheli, P., O. Haller, W. Boll, J. Lindenmann, and C. Weissmann.** 1986. Mx protein: constitutive expression in 3T3 cells transformed with cloned Mx cDNA confers selective resistance to influenza virus. Cell **44:**147–158.
51. **Staeheli, P., F. Pitossi, and J. Pavlovic.** 1993. Mx proteins: GTPases with antiviral activity. Trends Cell Biol. **31:**268–272.
52. **Stollar, V., R. W. Schlesinger, and T. M. Stevens.** 1967. Studies on the nature of dengue viruses. III. RNA synthesis in cells infected with type 2 dengue virus. Virology **33:**650–658.
53. **Szewczak, A. A., and P. B. Moore.** 1995. The sarcin/ricin loop, a modular RNA. J. Mol. Biol. **247:**81–98.
54. **Todd, S., J. H. Nguyen, and B. L. Semler.** 1995. RNA-protein interaction directed by the 3′ end of human rhinovirus genomic RNA. J. Virol. **69:**3605–3614.
55. **Vaheri, A., W. D. Sedwick, S. A. Plotkin, and R. Maes.** 1965. Cytopathic effect of rubella virus in BHK-21 cells and growth to high titers in suspension cultures. Virology **27:**239–241.
56. **Vainio, T.** 1963. Virus and hereditary resistance in vitro. I. Behavior of West Nile (E-101) virus in the cultures prepared from genetically resistant and susceptible strains of mice. Ann. Med. Exp. Biol. Fenn. **41:**1–24.
56a. **Vainio, T., R. Gavatkin, and H. Koprowski.** 1961. Production of interferon by brains of genetically resistant and susceptible mice infected with West Nile virus. Virology **14:**385–387.
57. **Webster, L. T.** 1923. Microbic virulence and host susceptibility in mouse typhoid infection. J. Exp. Med. **37:**231–244.
58. **Webster, L. T.** 1937. Inheritance of resistance of mice to enteric bacterial and neurotropic virus infections. J. Exp. Med. **65:**261–286.
59. **Weiser, W., I. Vellisto, and F. B. Bang.** 1976. Congenic strains of mice susceptible and resistant to mouse hepatitis virus. Proc. Soc. Exp. Biol. Med. **152:**499–502.
60. **Wimberly, B., G. Varani, and I. Tinoco, Jr.** 1993. The conformation of loop E of eukaryotic 5S ribosomal RNA. Biochemistry **32:**1078–1087.
61. **Zuo, E. T., F. A. Tanious, W. D. Wilson, G. Zon, G. S. Tan, and R. M. Wartell.** 1990. Effect of base-pair sequence on the conformations and thermally induced transitions in oligodeoxyribonucleotides containing only AT base pairs. Biochemistry **29:**4446–4456.